

Exact-exchange Kohn-Sham formalism applied to one-dimensional periodic electronic systemsStefan Rohra,¹ Eberhard Engel,² and Andreas Görling¹¹*Lehrstuhl für Theoretische Chemie, Universität Erlangen-Nürnberg, Egerlandstr. 3, D-91058 Erlangen, Germany*²*Institut für Theoretische Physik, J.W. Goethe-Universität Frankfurt, Max-von-Laue-Str. 1, D-60438 Frankfurt/Main, Germany*

(Received 14 December 2005; revised manuscript received 16 May 2006; published 21 July 2006)

The exact-exchange (EXX) Kohn-Sham formalism, which treats exchange interactions exactly within density-functional theory, is applied to one-dimensional periodic systems. The underlying implementation does not rely on specific symmetries of the considered system and can be applied to any kind of periodic structure in one to three dimensions. As a test system, *trans*-polyacetylene, both in the form of an isolated chain and in the bulk geometry has been investigated. Within the EXX scheme, bandstructures and independent particle response functions are calculated and compared to experimental data as well as to data calculated by several other methods. Compared to results from the local-density approximation, the EXX method leads to an increased value for the band gap, in line with similar observations for three-dimensional semiconductors. An inclusion of correlation potentials within the local density approximation or generalized gradient approximations leads to only negligible effects in the bandstructure. The EXX band gaps are in good agreement with experimental data for bulk *trans*-polyacetylene. Packing effects of the chains in bulk *trans*-polyacetylene are found to reduce the band gap by about 0.5 eV.

DOI: [10.1103/PhysRevB.74.045119](https://doi.org/10.1103/PhysRevB.74.045119)

PACS number(s): 71.20.Rv, 31.15.Ew, 71.15.-m, 78.30.Jw

I. INTRODUCTION

The bandstructure is the key quantity for studying the electronic structure of solids and of periodic systems in general. Presently, in most cases, Kohn-Sham (KS) bandstructures, calculated either within the local density approximation^{1,2} (LDA) or within some generalized gradient approximation (GGA),¹⁻³ represent the starting point for such investigations. In particular, the *GW* method,⁴⁻⁸ the currently most popular approach for the calculation of quasiparticle bandstructures and band gaps, is usually based on LDA or GGA bandstructures. While it is possible to perform fully self-consistent *GW* calculations, this is usually not done, because such calculations are not only computationally more demanding than the non-self-consistent treatment based on LDA or GGA one-particle states and eigenvalues, but also because in some of the few cases where such calculations have been carried out for solids worse results compared to experiment⁹ were obtained. While the non-self-consistent *GW* approach based on KS input is somewhat unsatisfactory from a formal point of view, its success nevertheless underlines the central role of the KS bandstructure. Moreover, also the methods to investigate optical properties usually start from the KS bandstructure, such as, for instance, the Bethe-Salpeter method^{8,10-13} or methods based on time-dependent density-functional theory¹⁴⁻¹⁹ or time-dependent current-density-functional theory.²⁰

Despite their central role for the investigation of electronic systems LDA and GGA bandstructures suffer from severe shortcomings. The most important of these is the substantial underestimation of the band gaps of semiconductors and insulators.²¹⁻²⁶ This fact was often attributed to the KS formalism itself. Indeed, even the exact KS band gap, i.e., the gap which would result from the exact KS exchange-correlation potential, is not identical with the physical band gap.^{21,22} The two gaps differ by the derivative discontinuity of the exchange-correlation potential at integer electron

numbers.^{21,22} As a matter of fact, KS orbitals and eigenvalues originally were considered as auxiliary quantities with no or little physical meaning. Recently, however, it was shown that KS eigenvalues and their differences are physically meaningful and, e.g., are well-defined zeroth order approximations for ionization and excitation energies²⁷⁻³² as well as for band gaps.³³ In order to clarify the meaning of these zeroth order approximations it is instructive to consider how excitation energies and band gaps are given in density-functional theory (DFT). Excitation energies result from time-dependent (TD) DFT. For excitation energies that refer to excitations from an occupied to an unoccupied orbital within a one-particle picture, TDDFT excitation energies can be considered as the sum of the corresponding eigenvalue difference plus a TDDFT correction. Band gaps, on the other hand, are given by the smallest eigenvalue difference between occupied and unoccupied orbitals, i.e., the KS band gap, plus the derivative discontinuity. At the level of the zeroth order approximation of KS eigenvalue differences, TDDFT corrections or derivative discontinuities, respectively, are neglected. Therefore optical absorption onsets, i.e., optical band gaps, related to excitation energies and quasiparticle band gaps including fundamental band gaps are not distinguished at the level of KS eigenvalue differences. Nevertheless, eigenvalue differences can be reasonable approximations for quasiparticle band gaps and excitation energies as discussed below.

The shortcomings of LDA and GGA bandstructures, at least in most cases, seem to predominantly originate from the exchange-correlation functionals used, rather than from limitations of the KS formalism itself. The major problem of the LDA and GGA is the incomplete cancellation of the unphysical self-interaction of each electron with itself, which is contained in the Coulomb energy and potential. These Coulomb self-interactions raise the KS eigenvalues. The more localized valence bands are affected more strongly than the less localized conduction bands. As a result of the different impact of the self-interaction error on valence and conduction bands the LDA or GGA band gaps are artificially de-

creased. While, in principle, the self-interaction contained in the Coulomb potential is exactly cancelled by the KS exchange potential, the LDA and GGA for the latter not nearly lead to a complete cancellation.

Recently, a KS approach for solids treating the exchange energy and potential exactly was introduced.^{34–37} This exact-exchange (EXX) approach does not suffer from the spurious self-interaction and yields band gaps that are much larger than those from LDA or GGA calculations. For standard semiconductors band gaps in excellent agreement with experiment were obtained.^{36–40} In these calculations the correlation potential was either completely neglected or approximated within the LDA or GGAs. It turned out that the choice of the treatment of the correlation potential has little effect on the bandstructure. The agreement between experimental and EXX band gaps for standard semiconductors shows that for these materials the approximations made in the EXX approach, the neglect of the derivative discontinuity and the approximate treatment of the correlation potential together have little effect. For these materials the EXX approach therefore is an alternative to the *GW* method. The EXX approach, from a formal point of view, has the advantage that it is a pure KS procedure, which is carried out self-consistently. Furthermore, the more physical EXX band structures can be used instead of LDA or GGA bandstructures as basis of *GW*,^{41,42} Bethe-Salpeter, or time-dependent density-functional methods.¹⁹

Note that EXX band structures, even in the exchange-only case, are completely different from Hartree-Fock (HF) band structures. Both exact exchange-only KS and HF methods treat exchange exactly, however, the underlying exchange energy and potential are defined differently. The exchange energy in both cases is the exchange energy of the corresponding Slater determinant, the HF determinant, or the KS determinant, respectively. However, the latter two determinants, and therefore also the orbitals building them, are different and subsequently also the HF and exchange-only KS exchange energies are different. The HF and KS orbitals and thus the corresponding determinants are different because the HF and exchange-only KS one-particle equations contain a different exchange potential. The KS exchange potential is defined as the functional derivative of the exchange energy with respect to the electron density and therefore, by definition, is a local multiplicative potential. The local multiplicative KS exchange potential acts in the same way on all orbitals, be they occupied or unoccupied. The exact exchange potential therefore cancels the unphysical Coulomb self-interactions contained in the Coulomb potential for all orbitals. The nonlocal HF exchange potential acts in a different way on occupied and unoccupied orbitals and as a result only the occupied orbitals are unaffected by Coulomb self-interactions and describe electrons in the system under consideration. The unoccupied orbitals, on the other hand, describe electrons in the corresponding $N+1$ -particle system with N being the number of electrons. As a result HF band structures usually exhibit a much too large band gap and in case of metals a singularity at the Fermi level. Exact exchange-only KS bandstructures, on the other hand, are not affected by such problems.

While EXX methods yield very good results for standard semiconductors, an EXX study of solid noble gases leads to

a somewhat mixed picture.⁴³ The calculated band gaps are clearly superior to the LDA values, but are still significantly below the experimental data. So far, EXX methods were only applied to three-dimensional periodic systems (as well as to atoms⁴⁴ and molecules^{45,46}). It seems desirable to investigate the performance of EXX methods also for other types of periodic systems. In this work the EXX approach is applied to the electronic structure of *trans*-polyacetylene, as a typical representative of an organic one-dimensional periodic system. One-dimensional organic oligomers or polymeres are of great interest due to their high potential as active materials in new optoelectronic devices.

Trans-polyacetylene is the prototype example for an organic one-dimensional periodic system. While an isolated *trans*-polyacetylene chain may be considered as a molecular wire or one-dimensional semiconductor, in practice usually fibers of *trans*-polyacetylene or crystalline bulk *trans*-polyacetylene are encountered.^{47,48} Despite the fact that crystalline *trans*-polyacetylene is a three-dimensional periodic material its properties are mostly determined by the periodicity along the polyacetylene chain. We therefore occasionally address all forms of *trans*-polyacetylene as one-dimensional periodic materials in this work despite the fact that it is shown below that there exists some nonnegligible packing effects in crystalline *trans*-polyacetylene. Because *trans*-polyacetylene is a prototypical one-dimensional periodic organic system it is not surprising that a number of theoretical studies of the optical properties of this system have been carried out.^{49–55} In Ref. 53 the band gap and the optical spectrum of an isolated *trans*-polyacetylene chain were calculated with the *GW* and the Bethe-Salpeter method, respectively. The results, e.g., the band gap of 2.1 eV and the absorption spectrum with a single peak at 1.7 eV, agree well with experimental data,^{56,57} which, however, refer to bulk *trans*-polyacetylene. In Ref. 55, on the other hand, a much larger band gap of 4.1 eV for an isolated *trans*-polyacetylene chain was obtained by a multireference configuration interaction approach. Finally, in Refs. 51 and 54, band gaps of 3.96 and 3.68 eV, respectively, emerged from Møller-Plesset perturbation theory for an isolated *trans*-polyacetylene chain. As most of these studies considered isolated chains, but relied on experimental data from bulk polyacetylene for comparisons, it seems desirable to investigate the influence of the geometry and the arrangement of polyacetylene chains on the bandstructure. Such an investigation is the second goal of this work, besides the assessment of the performance of the EXX approach for one-dimensional periodic organic systems.

II. METHOD

Within the EXX KS approach,^{34–37,44,58–62} the exchange energy as well as the local multiplicative KS exchange potential, not to be confused with the nonlocal Hartree-Fock exchange potential, are treated exactly, rather than via some approximate density functional. For a periodic system the exact exchange energy per unit cell is given by

$$E_x(\mathbf{r}) = -(1/N_{\mathbf{k}}) \times \sum_{vv'\mathbf{k}\mathbf{k}'} \int \int d\mathbf{r}d\mathbf{r}' \frac{\phi_{v\mathbf{k}}^*(\mathbf{r})\phi_{v'\mathbf{k}'}(\mathbf{r})\phi_{v'\mathbf{k}'}^*(\mathbf{r}')\phi_{v\mathbf{k}}(\mathbf{r}')}{|\mathbf{r}-\mathbf{r}'|}. \quad (1)$$

In Eq. (1), $\phi_{v\mathbf{k}}$ are valence orbitals, with crystal momentum \mathbf{k} . Orbitals generally are assumed to be normalized with respect to the crystal volume. In the considered case of non-spin-polarized systems, the occupied orbitals are doubly occupied and spin is taken into account by appropriate prefactors of 2. The summation runs over all valence bands, v and v' , and over all \mathbf{k} points \mathbf{k} and \mathbf{k}' within the first Brillouin zone. The number of \mathbf{k} points is denoted by $N_{\mathbf{k}}$.

The KS exchange potential v_x is defined as the functional derivative $v_x(\mathbf{r}) = \delta E_x[\rho]/\delta\rho(\mathbf{r})$ of the exchange energy with respect to the electron density. It obeys the equation

$$\int d\mathbf{r}' X_s(\mathbf{r},\mathbf{r}')v_x(\mathbf{r}') = 2 \sum_{v\mathbf{c}\mathbf{k}} \left[\langle v\mathbf{k} | \hat{v}_x^{\text{NL}} | \mathbf{c}\mathbf{k} \rangle \frac{\phi_{\mathbf{c}\mathbf{k}}^*(\mathbf{r})\phi_{v\mathbf{k}}(\mathbf{r})}{\epsilon_{v\mathbf{k}} - \epsilon_{\mathbf{c}\mathbf{k}}} + \text{c.c.} \right], \quad (2)$$

which shall be called EXX equation. The $\phi_{\mathbf{c}\mathbf{k}}$ occurring on the right hand side of the EXX equation are unoccupied orbitals forming conduction bands c and the nonlocal operator \hat{v}_x^{NL} with the kernel

$$\hat{v}_x^{\text{NL}}(\mathbf{r},\mathbf{r}') = - \sum_{v\mathbf{q}} \frac{\phi_{v\mathbf{q}}(\mathbf{r})\phi_{v\mathbf{q}}^*(\mathbf{r}')}{|\mathbf{r}-\mathbf{r}'|} \quad (3)$$

is a nonlocal exchange operator of the form of the Hartree-Fock exchange operator, but built from KS orbitals. The eigenvalues of the orbitals $\phi_{v\mathbf{k}}$ and $\phi_{\mathbf{c}\mathbf{k}}$ are denoted by $\epsilon_{v\mathbf{k}}$ and $\epsilon_{\mathbf{c}\mathbf{k}}$, respectively. The independent particle response function X_s , i.e., the response function of the KS system, is given by

$$X_s(\mathbf{r},\mathbf{r}') = \frac{\delta\rho(\mathbf{r})}{\delta v_s(\mathbf{r}')} = 2 \sum_{v\mathbf{c}\mathbf{k}} \frac{\phi_{v\mathbf{k}}^*(\mathbf{r})\phi_{\mathbf{c}\mathbf{k}}(\mathbf{r})\phi_{\mathbf{c}\mathbf{k}}^*(\mathbf{r}')\phi_{v\mathbf{k}}(\mathbf{r}')}{\epsilon_{v\mathbf{k}} - \epsilon_{\mathbf{c}\mathbf{k}}} + \text{c.c.} \quad (4)$$

In Eq. (4), v_s is the effective KS potential.

If the exchange potential v_x , the response function X_s , and the right hand side of the EXX equation (2) are expanded in an auxiliary basis set, here an auxiliary plane wave basis set, then the EXX equation turns into a matrix equation, which can easily be handled computationally.³⁵⁻³⁷

III. COMPUTATIONAL DETAILS

Originally the EXX formalism was implemented in a plane-wave code optimized for three-dimensional periodic cubic systems³⁷ by exploiting the cubic symmetry and by using the concept of special \mathbf{k} points.^{63,64} For the investigation of noncubic systems, including one- or two-dimensional periodic systems via the super cell ansatz, we programmed a new plane-wave implementation, which does not rely on symmetry or special \mathbf{k} points. In supercell calculations we treat the directions along the artificial periodicity due to the supercell ansatz similar to the other direction related to real

physical periodicity in the sense that no other plane wave cutoffs or artificial screenings are introduced. Merely, the number of \mathbf{k} points is set to one for those directions in the Brillouin zone that correspond to the directions along the artificial periodicity. In order to test that the super cells were chosen large enough we additionally carried out calculations with more than one \mathbf{k} point along the directions corresponding to the artificial periodicity and checked that results did not change and, in particular, that no significant dispersion occurred in those directions.

The cutoff for the plane wave basis set to represent the orbitals and the cutoff for the auxiliary plane wave basis set representing the KS response function X_s and the exchange potential v_x in all cases were chosen to be 32 and 12 Ry, respectively. While these cutoffs are not sufficient for calculations of total energies, they turned out to be sufficient for the calculation of bandstructures. Errors in the resulting band gaps can be estimated to be below the order of about 0.05 eV, which is more than sufficient for the purpose of this work.

Instead of special \mathbf{k} points, we used uniform grids of \mathbf{k} points covering the first Brillouin zone. For self-consistent KS calculations of isolated chains of polyacetylene we used 24 \mathbf{k} points in the direction of the chain, which ensured very good convergence with the number of \mathbf{k} points. For self-consistent KS calculations of bulk *trans*-polyacetylene additional \mathbf{k} points were placed in the two directions along the reciprocal unit cell vectors not corresponding to the chain direction. Here, a uniform $2 \times 32 \times 2$ mesh (32 \mathbf{k} -points along the chain direction, 2 \mathbf{k} points along the two other directions) was employed. The calculations of bandstructures and KS response functions, as usually, are based on the KS potentials obtained in the self-consistent calculations, i.e., the band structures and KS response functions were calculated by diagonalizing, for the required \mathbf{k} points, KS Hamiltonian operators containing the KS potentials from the self-consistent calculations. (Note that the exact KS exchange potential, in contrast to the HF exchange potential, does not depend on the crystal momentum \mathbf{k} of the orbital it acts upon.) For the KS response functions of isolated chains of polyacetylene we used a uniform $1 \times 350 \times 1$ mesh of \mathbf{k} points, for bulk *trans*-polyacetylene a uniform $5 \times 150 \times 5$ mesh was employed.

In all calculations all unoccupied states were taken into account for both the construction of the response function and the right hand side of the EXX equation. Typical values for the number of conduction bands were 3600 (1500) for the isolated chain (bulk) case.

In the case of EXX calculations the use of pseudopotentials is particularly attractive in view of the large number of Fock matrix elements to be evaluated in all-electron calculations. For that reason EXX pseudopotentials have been introduced quite early.^{36,37,65,66} However, it has been noticed immediately that a spurious long-range structure develops in the EXX pseudopotential,^{36,37,65,66} if the standard procedure for the construction of normconserving pseudopotentials⁶⁷⁻⁶⁹ is utilized. This long-range structure, which effectively simulates an additional artificial charge on the ion, can be traced to the core-valence interaction.⁷⁰ In order to eliminate this structure in a systematic fashion a self-consistent pseudopo-

tential construction scheme has been introduced,⁷⁰ in which a clean asymptotic behavior is enforced as a constraint. The resulting EXX pseudopotentials have been shown to give very accurate atomic excitation energies and spectroscopic constants of molecules. In Ref. 70 it has also been demonstrated explicitly that, apart from the long-range structure eliminated via the self-consistent pseudopotential construction, the core-valence interaction is less relevant in the case of the exact exchange than for the LDA.

In the present work, all calculations with the exact exchange were based on normconserving pseudopotentials obtained by this self-consistent pseudopotential construction scheme. In all cases the density-functionals (LDA, exact exchange only, exact exchange plus approximate correlation) used for the generation of the pseudopotentials and in the self-consistent ground-state calculations of the periodic system were chosen to be identical (pure LDA pseudopotentials were generated by the standard procedure⁶⁹). For hydrogen the pseudopotentials contained exclusively an angular momentum component with $l=0$. For carbon pseudopotentials with s and p components were employed, with the s component chosen as local component for all calculations. Additional tests with the p component as local component for the carbon atom were carried out, but did not lead to significant changes of the results. For the cutoff radii of the pseudopotentials values of $r_{c,l=0}^H=0.9$, $r_{c,l=0}^C=1.2$, and $r_{c,l=1}^C=1.1$ (in units of Bohr radii) were used, following Ref. 70.

IV. RESULTS

A. Isolated, infinite chain of *trans*-polyacetylene

As a first system we consider an isolated, infinite chain of *trans*-polyacetylene, relying on the supercell concept. The polymere is planar and exhibits alternating single and double bonds between the carbon atoms, which are accompanied by different bondlengths. The unit cell contains a C_2H_2 unit. The bond distances of the carbon backbone were taken from experimental data from x-ray scattering of crystalline *trans*-polyacetylene.⁴⁷ This geometry, which shall be named G1, has also been used in a recent investigation of electronic correlation effects in *trans*-polyacetylene.⁵⁵ The carbon-carbon bond lengths in geometry G1 are given by $d(C-C)=1.45$ Å and $d(C=C)=1.36$ Å. The lattice constant along the chain direction equals 2.455 Å.⁴⁸ A (C—H) bondlength of 1.087 Å has been found by optimization on the HF and MP2 level.⁵⁰ The angle $\angle(C-C, C=C)$ [with respect to the short (C=C) double bond] has been determined to be 120.057° via HF optimization.⁵⁵

The system was placed in the the xy plane with the chain oriented along the y direction. The unit cell is defined by the vectors $\mathbf{a}_1=(a,0,0)$, $\mathbf{a}_2=(0,c,0)$, and $\mathbf{a}_3=(a/2,0,b)$ with the parameter $c=2.455$ Å defining the lattice vector along the polyacetylene chain. The parameter a was set to $a=8$ Å. The third lattice vector was chosen in a way that the

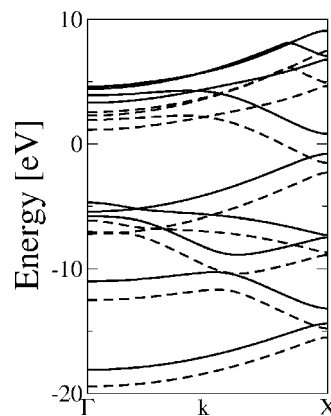


FIG. 1. Bandstructure for an isolated, infinite chain of polyacetylene for the LDA (dashed lines) and the EXX (solid lines) case.

p orbitals of the carbon atoms of two adjacent chains do not lie on top of each other, but at maximal distance. The parameter b was set to $b=9$ Å. The values of $a=8$ Å and $b=9$ Å turned out to be large enough that the chains can be considered as isolated. Effects on the band gap due to coupling of the chains can be estimated by variation of the supercell size to be below 0.05 eV. For further details of the geometry see the Appendix.

The calculated LDA band gap equals 0.78 eV, whereas the EXX calculation yields a band gap of 1.63 eV. The bandstructure for these two cases is displayed in Fig. 1, adjusted with respect to each other by placing the Fermi energy at 0 eV. The LDA and EXX bandstructure are qualitatively similar, however, the energetical difference between valence and conduction bands is significantly smaller in the case of the LDA, leading to the observed small gap. This is in line with the finding that for three-dimensional semiconductors the EXX approach increases the commonly too small LDA band gap. Addition of an LDA correlation potential to the EXX potential leads to a band gap of 1.65 eV, i.e., increases the gap marginally by 0.01 eV, whereas addition of a GGA-correlation potential, here the PBE correlation potential, to the EXX potential marginally decreases the gap to 1.61 eV. This shows, again in line with the observation for three-dimensional semiconductors, that the treatment of the correlation potential has no significant influence on the band gap. Within the EXX scheme, the band gap comes close to the value of 2.1 eV resulting from *GW* calculations,⁵³ but still stays somewhat smaller. The calculated band gaps as well as those from several other methods are collected in Table I.

To investigate the sensitivity of the bandstructure of an isolated polyacetylene chain on the geometry, we calculated the EXX bandstructure also in a slightly modified geometry, denoted G2, which has also been used in Ref. 53. The geometry G2 is characterized by the carbon-carbon bondlengths $d(C-C)=1.44$ Å and $d(C=C)=1.36$ Å.⁷¹ Optimization yielded⁵³ a lattice constant along the chain direction of 2.473 Å. A carbon hydrogen bond length $d(C-H)=1.1$ Å (Ref. 53) and an angle $\angle(C-C, C=C)$ of 118° have been used (see also the Appendix). In geometry G2 an EXX band gap of 1.56 eV is obtained, which differs only slightly from the result observed for the geometry G1.

TABLE I. Bandgaps (in eV) for an isolated, infinite chain of *trans*-polyacetylene calculated with various density functionals, the EXX case has been calculated for the two different geometries G1 and G2. For comparison, values of Hartree-Fock (HF), Møller-Plesset theory (MP2), multireference configuration interaction (MRCI), and quasiparticle calculations (*GW*) are given as well.

	X
HF	6.06 ^a
MP2	3.68 ^a , 3.96 ^b
MRCI	4.11 ^c
GW	2.1 ^d
LDA(G1)	0.78
EXX(G1)	1.62
EXX(G2)	1.56
EXX-VWN(G1)	1.65
EXX-PBE(G1)	1.61

^aRef. 54.

^bRef. 51.

^cRef. 55.

^dRef. 53.

B. Bulk *trans*-polyacetylene

The geometries of the chains building the considered bulk *trans*-polyacetylene are those of the above discussed isolated chains in geometry G1, i.e., the geometry based on the x-ray structure.⁴⁸ Within the crystalline *trans*-polyacetylene, each unit cell contains two polyacetylene chains. The unit cell according to Ref. 47 corresponds to a simple monoclinic Bravais lattice with the values of $a=4.24$ Å, $b=7.32$ Å, and $c=2.46$ Å for the lattice constants (see the Appendix for further details).

Again we carried out LDA and EXX calculations, which yielded band gaps at the X point of 0.98 and 1.64 eV. The corresponding bandstructures are displayed in Figs. 2 and 3. However in both cases the band gap at the X point is not the fundamental band gap. Along the line from the Γ to the X point, one observes band gaps (0.81 eV for LDA and 1.55 eV for EXX), which are reduced in comparison to the

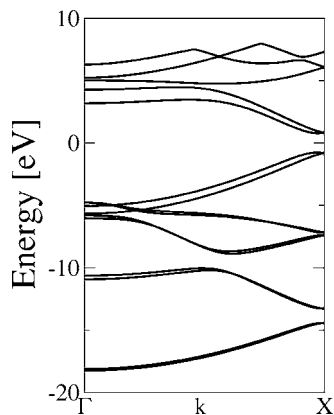


FIG. 2. Bandstructure for bulk polyacetylene for the EXX case.

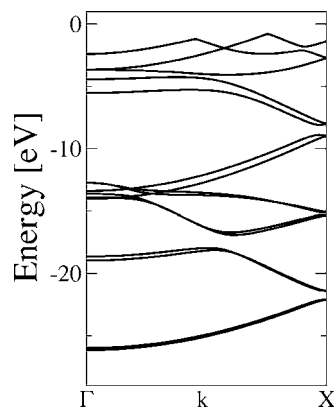


FIG. 3. Bandstructure for bulk polyacetylene for the LDA case.

gaps at the X point. However, this band gap also is not the fundamental band gap. For LDA as well as EXX calculations, the smallest band gaps we found are located at the point (0.5,0.5,0.0), in multiples of the reciprocal lattice vectors (see Appendix for numbering of reciprocal lattice vectors), i.e., at the edge of the Brillouin zone. At this point we calculated band gaps of 0.43 eV for LDA and 1.18 eV for EXX, which represent, compared to the band gap at the X point, a remarkable dispersion of about 0.55 eV for LDA, respectively, 0.46 eV for EXX. This finding is in agreement with results from Hartree-Fock calculations which estimated a reduction of the band gap by 0.6 eV due to interband interactions.⁵⁵ The LDA and EXX bandstructures along the line from point (0.5,0.5,0.0) to point (0.5,0.5,0.5) in multiples of the reciprocal lattice vectors are shown in Figs. 4 and 5.

Furthermore, we also checked the influence of the addition of an LDA or PBE correlation potential to the EXX potential. As in the case of the isolated chain, the correlation potential turned out to have an only negligible effect on the bandstructure.

Optical absorption experiments for *trans*-polyacetylene in the considered geometry⁵⁶ give an absorption coefficient rising sharply at 1.4 eV and having a peak at about 1.9 eV. A

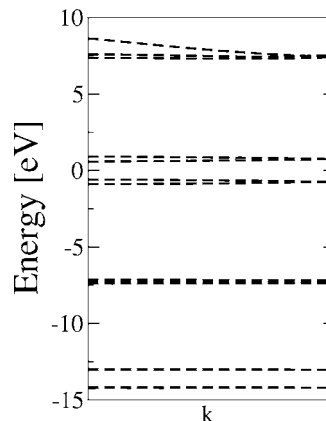


FIG. 4. Dispersion of the band gap for bulk polyacetylene (EXX case) along the line from point (0.5,0.5,0.0) to point (0.5,0.5,0.5) in multiples of the reciprocal lattice vectors.

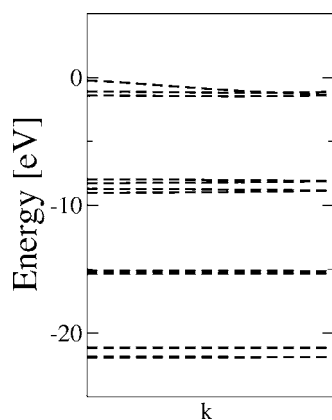


FIG. 5. Dispersion of the band gap for bulk polyacetylene (LDA case) along the line from point (0.5,0.5,0.0) to point (0.5,0.5,0.5) in multiples of the reciprocal lattice vectors.

second similar measurement⁵⁷ gives an identical value for the peak and a value of 1.5 eV for the onset of the absorption. The lattice constants mentioned within the framework of this second measurement,⁴⁸ differ slightly from the geometry of Ref. 56, underlying our calculations ($a=4.18$ Å, $b=7.34$ Å, $c=2.455$ Å). Nevertheless, the experimental results for the two distinct measurements agree more or less and are in reasonable agreement with the band gaps from our EXX calculations. (Remember that no distinction between quasiparticle and optical band gaps is made at the level of a zeroth order approximation relating KS eigenvalue differences to observables.) The data of the band gaps for all discussed cases have been compiled in Table II.

C. Reponse functions

The optical absorption strength obtained by the independent particle, i.e., Kohn-Sham, response function for an isolated *trans*-polyacetylene chain in geometry G1 is shown in Fig. 6 for the EXX case. The onset of the peak coincides with the calculated fundamental band gap, the absorption

TABLE II. Bandgaps (in eV) for bulk-*trans*-polyacetylene. In addition to the value for the gap at the X point of the Brillouin zone, a smaller gap between the Γ and the X point ($X \rightarrow \Gamma$) has been observed. The smallest gap was found at the point (0.5, 0.5, 0.0) (in units of the reciprocal lattice vectors) lying on the edge of the Brillouin zone. The experimental values of the band gap correspond to the energy, where a sharp rise in the absorption spectrum is observed, i.e., to the optical gap.

	Δ_X	$\Delta_{X \rightarrow \Gamma}$	Δ_{\min}
LDA	0.98	0.81	0.43
EXX	1.64	1.55	1.18
EXX-VWN	1.65	1.57	1.21
EXX-PBE	1.61	1.52	1.17
Experiment			1.4 ^a , 1.5 ^b

^aRef. 56.

^bRef. 57.

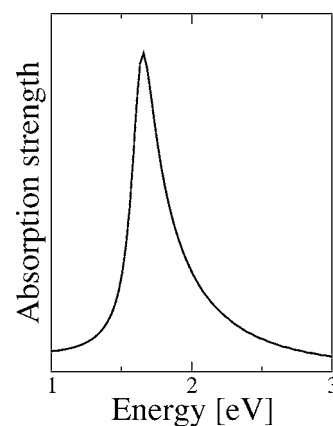


FIG. 6. EXX Kohn-Sham response function for an isolated, infinite chain of polyacetylene.

maximum lies about 0.1 eV higher than the band gap. A similar behavior was obtained for the Kohn-Sham response function for the LDA case with the corresponding peak shifted to a lower energy. The absorption spectrum resulting from the EXX response function is quite similar to the one obtained via the Bethe-Salpeter equation,⁵³ which includes electron-hole interactions, i.e., excitonic effects, that are missing in an independent particle spectrum. This could be due to a cancellation of two effects. For an isolated *trans*-polyacetylene chain the neglect of electron-hole interactions seems to shift⁵³ the peak of the absorption spectrum to higher energy values. This could cancel the effect that the EXX band gap is smaller than the one obtained within the *GW* scheme.⁵³ In any case the similarity between the Bethe-Salpeter and the EXX absorption spectra suggests that, beyond a possible shift of the spectrum, electron-hole interactions have little effect on the optical spectrum of isolated polyacetylene chains. The absorption spectrum of the isolated chain obtained via the Bethe-Salpeter equation agrees quite well with the experimental spectrum observed for bulk *trans*-polyacetylene. However, in the previous subsection we showed that packing effects in the bulk reduce the fundamental band gap by about 0.5 eV. Therefore it remains to be seen whether Bethe-Salpeter calculations for bulk *trans*-polyacetylene would yield an absorption spectrum in agreement with experiment or a spectrum shifted to lower energy.

The optical absorption spectrum resulting from the EXX independent particle response function for bulk *trans*-polyacetylene is displayed in Fig. 7. With a value of about 1.6 eV, the maximum of the response function lies close to the calculated values of the two band gaps at the X point and on the path between the X and the Γ point (see Table II). Compared to the Kohn-Sham response function for the case of an isolated, infinite chain of *trans*-polyacetylene, the displayed result for the bulk shows a broader peak. This widened shape, as well as the maximum position at about 1.6 eV is in agreement with the experimental data for bulk *trans*-polyacetylene.^{56,57}

V. CONCLUSIONS

The exact exchange KS approach, implemented within a plane wave pseudopotential framework, was shown to yield

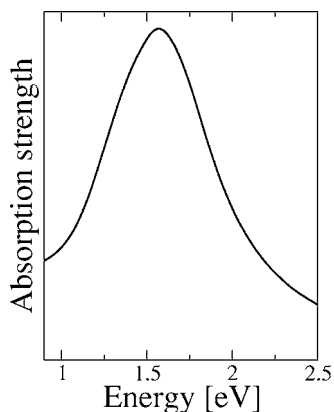


FIG. 7. EXX Kohn-Sham response function for bulk polyacetylene.

band gaps for a typical one-dimensional periodic organic polymere, which agree well with experimental data and with data obtained from *GW* methods and methods based on the Bethe-Salpeter equation. Similar to the case of three-dimensional periodic semiconductors, EXX band gaps are substantially larger than their LDA or GGA counterparts and thus closer to experiment. The EXX approach therefore promises to be a viable tool for the investigation of the electronic structure of organic polymeres, a class of materials with high potential as the active compound in new optoelectronic devices.

The findings of this work suggest that also for polyacetylene EXX band gaps are close to experimental band gaps, although in this case no direct measurements of fundamental

band gaps seem to be available and only comparisons between the EXX band gap and the optical band gap of bulk *trans*-polyacetylene can be made. EXX band gaps differ from the exact gaps only by the derivative discontinuity of the exchange-correlation potential and the contribution of the correlation potential. As in the case of semiconductors, the inclusion of an LDA or GGA correlation potential has little impact on the bandstructure, which suggests that quite generally the effect of the correlation potential can be considered to be negligible. Taken this for granted and assuming that fundamental and optical band gap of bulk *trans*-polyacetylene are not grossly different, the agreement of EXX and experimental band gaps implies that also the derivative discontinuity of the exchange-correlation potential is small. However, this point needs further investigation, because it could be that all presently available approximate correlation potentials are missing features that affect the bandstructure.

An important outcome of the present investigation is the fact that packing effects in bulk *trans*-polyacetylene have a substantial quantitative impact on the bandstructure: The band gap in bulk *trans*-polyacetylene is about 0.5 eV smaller than the one obtained for isolated chains. In future investigations of organic polymeres such packing effects therefore should be taken into account.

ACKNOWLEDGMENTS

We thank U. Birkenheuer and M. Rohlfing for providing the detailed geometry data underlying their calculations. This work was supported by the Deutsche Forschungsgemeinschaft. Calculations were carried out at the John-von-Neumann Institute of Computing.

APPENDIX

In Tables III–V displayed in this Appendix the geometric data for all considered systems is compiled. Positions (p, q, r) within the Brillouin zone are given in multiples $p\mathbf{b}_1 + q\mathbf{b}_2 + r\mathbf{b}_3$ of reciprocal lattice vectors \mathbf{b}_1 , \mathbf{b}_2 , and \mathbf{b}_3 within the main text. The reciprocal lattice vectors \mathbf{b}_1 , \mathbf{b}_2 , and \mathbf{b}_3 correspond to the lattice vectors \mathbf{a}_1 , \mathbf{a}_2 , and \mathbf{a}_3 , respectively. The vectors \mathbf{a}_2 and \mathbf{b}_2 are associated with the direction of the polyacetylene chains.

TABLE III. Geometric data for bulk *trans*-polyacetylene given in atomic units. Realspace unit cell vectors are denoted as \mathbf{a}_i , coordinates of hydrogen (carbon) atoms are denoted as H_i (C_i).

	x	y	z
\mathbf{a}_1	8.01244060	0.0	0.0
\mathbf{a}_2	-0.12144217	4.63768905	0.0
\mathbf{a}_3	0.0	0.0	13.83279947
H_1	-1.76389103	-1.153571655	-5.367986055
H_2	-2.18160819	-1.165272865	1.548413675
H_3	2.18160821	1.165272865	-1.548413665
H_4	1.88533319	-3.484117395	5.367986055
C_1	-3.44604796	-1.194232545	-6.546186695
C_2	-0.49945126	-1.124611975	0.370213055
C_3	0.49945126	1.124611975	-0.370213055
C_4	3.56749012	-3.443456505	6.546186695

TABLE IV. Geometric data for isolated chain of *trans*-polyacetylene (geometry $G1$) given in atomic units. Realspace unit cell vectors are denoted as \mathbf{a}_i , coordinates of hydrogen (carbon) atoms are denoted as H_i (C_i).

	x	y	z
\mathbf{a}_1	15.11781328	0.0	0.0
\mathbf{a}_2	0.0	4.63927896	0.0
\mathbf{a}_3	7.55890664	0.0	17.00753994
H_1	-2.69959124	1.10770723	0.0
H_2	2.69959124	-1.10770723	0.0
C_1	-0.64546122	1.11114406	0.0
C_2	0.64546122	-1.11114406	0.0

TABLE V. Geometric data for isolated chain of *trans*-polyacetylene (geometry $G2$) given in atomic units. Realspace unit cell vectors are denoted as \mathbf{a}_i , coordinates of hydrogen (carbon) atoms are denoted as H_i (C_i).

	x	y	z
\mathbf{a}_1	15.11781328	0.0	0.0
\mathbf{a}_2	0.0	4.67329404	0.0
\mathbf{a}_3	7.55890664	0.0	17.00753994
H_1	-2.69868711	1.24389067	0.0
H_2	2.69850018	-1.24389067	0.0
C_1	-0.61981899	1.21122435	0.0
C_2	0.61981899	-1.21122435	0.0

- ¹R. G. Parr and W. Yang, *Density-Functional Theory of Atoms and Molecules* (Oxford University Press, Oxford, 1989).
- ²R. M. Dreizler and E. K. U. Gross, *Density Functional Theory* (Springer, Heidelberg, 1990).
- ³W. Koch and M. C. Holthausen, *A Chemist's Guide to Density Functional Theory* (Wiley-VCH, New York, 2000).
- ⁴L. Hedin, Phys. Rev. **139**, A796 (1965).
- ⁵M. S. Hybertsen and S. G. Louie, Phys. Rev. Lett. **55**, 1418 (1985).
- ⁶F. Aryasetiawan and O. Gunnarsson, Rep. Prog. Phys. **61**, 237 (1998).
- ⁷W. G. Aulbur, L. Jönsson, and J. W. Wilkins, Solid State Phys. **54**, 1 (2000).
- ⁸G. Onida, L. Reining, and A. Rubio, Rev. Mod. Phys. **74**, 601 (2002).
- ⁹W. D. Schöne and A. G. Eguiluz, Phys. Rev. Lett. **81**, 1662 (1998).
- ¹⁰W. Hanke and L. J. Sham, Phys. Rev. Lett. **43**, 387 (1979).
- ¹¹S. Albrecht, L. Reining, R. DelSole, and G. Onida, Phys. Rev. Lett. **80**, 4510 (1998).
- ¹²L. X. Benedict, E. L. Shirley, and R. B. Bohn, Phys. Rev. Lett. **80**, 4514 (1998).
- ¹³M. Rohlfing and S. G. Louie, Phys. Rev. Lett. **81**, 2312 (1998).
- ¹⁴E. Runge and E. K. U. Gross, Phys. Rev. Lett. **52**, 997 (1984).
- ¹⁵E. K. U. Gross, J. F. Dobson, and M. Petersilka, in *Density Functional Theory II*, Springer Series in Topics in Current Chemistry, Band 181, edited by R. F. Nalewajski (Springer, Heidelberg, 1996), p. 81.
- ¹⁶M. E. Casida, in *Recent Advances in Density Functional Methods*, Band I, edited by D. P. Chong (World Scientific, Singapore, 1995), p. 155.
- ¹⁷A. Görling, Int. J. Quantum Chem. **69**, 265 (1998).
- ¹⁸A. Görling, H. H. Heinze, S. P. Ruzankin, M. Staufer, and N. Rösch, J. Chem. Phys. **110**, 2785 (1999).
- ¹⁹Y.-H. Kim and A. Görling, Phys. Rev. Lett. **89**, 096402 (2002).
- ²⁰J. A. Berger, P. L. de Boeij, and R. van Leeuwen, Phys. Rev. B **71**, 155104 (2005).
- ²¹J. P. Perdew and M. Levy, Phys. Rev. Lett. **51**, 1884 (1983).
- ²²L. J. Sham and M. Schlüter, Phys. Rev. Lett. **51**, 1888 (1983).
- ²³C. Filippi, D. J. Singh, and C. J. Umrigar, Phys. Rev. B **50**, 14947 (1994).
- ²⁴G. Ortiz, Phys. Rev. B **45**, 11328 (1992).
- ²⁵L. J. Sham and M. Schlüter, Phys. Rev. B **32**, 3883 (1985).
- ²⁶J. P. Perdew, Int. J. Quantum Chem. **19**, 497 (1986).
- ²⁷J. P. Perdew, R. G. Parr, M. Levy, and J. L. Balduz, Phys. Rev. Lett. **49**, 1691 (1982).
- ²⁸C. O. Almbladh and U. von Barth, Phys. Rev. B **31**, 3231 (1985).
- ²⁹D. P. Chong, O. V. Gritsenko, and E. J. Baerends, J. Chem. Phys. **116**, 1760 (2002).
- ³⁰O. V. Gritsenko and E. J. Baerends, J. Chem. Phys. **117**, 9154 (2002).
- ³¹A. Görling, Phys. Rev. A **54**, 3912 (1996).
- ³²C. Filippi, C. J. Umrigar, and X. Gonze, J. Chem. Phys. **107**, 9994 (1997).
- ³³A. Görling and M. Levy, Phys. Rev. A **52**, 4493 (1995).
- ³⁴T. Kotani, Phys. Rev. Lett. **74**, 2989 (1995).

- ³⁵A. Görling, Phys. Rev. B **53**, 7024 (1996); **59**, 10370(E) (1999).
- ³⁶M. Städele, J. A. Majewski, P. Vogl, and A. Görling, Phys. Rev. Lett. **79**, 2089 (1997).
- ³⁷M. Städele, M. Moukara, J. A. Majewski, P. Vogl, and A. Görling, Phys. Rev. B **59**, 10031 (1999).
- ³⁸A. Qteish, A. I. Al-Sharif, M. Fuchs, M. Scheffler, S. Boeck, and J. Neugebauer, Comput. Phys. Commun. **169**, 28 (2005).
- ³⁹P. Rinke, A. Qteish, J. Neugebauer, C. Freysoldt, and M. Scheffler, New J. Phys. **7**, 126 (2005).
- ⁴⁰S. Sharma, J. K. Dewhurst, and C. Ambrosh-Draxl, Phys. Rev. Lett. **95**, 136402 (2005).
- ⁴¹W. G. Aulbur, M. Städele, and A. Görling, Phys. Rev. B **62**, 7121 (2000).
- ⁴²A. Fleszar, Phys. Rev. B **64**, 245204 (2001).
- ⁴³R. J. Magyar, A. Fleszar, and E. K. U. Gross, Phys. Rev. B **69**, 045111 (2004).
- ⁴⁴J. D. Talman and W. F. Shadwick, Phys. Rev. A **14**, 36 (1976).
- ⁴⁵A. Görling, Phys. Rev. Lett. **83**, 5459 (1999).
- ⁴⁶S. Ivanov, S. Hirata, and R. J. Bartlett, Phys. Rev. Lett. **83**, 5455 (1999).
- ⁴⁷C. R. Fincher Jr., C. E. Chen, A. J. Heeger, A. G. MacDiarmid, and J. B. Hastings, Phys. Rev. Lett. **48**, 100 (1982).
- ⁴⁸H. Kahlert, O. Leitner, and G. Leising, Synth. Met. **17**, 467 (1987).
- ⁴⁹C.-M. Liegener, J. Chem. Phys. **88**, 6999 (1988).
- ⁵⁰S. Suhai, Int. J. Quantum Chem. **42**, 193 (1992).
- ⁵¹J. Q. Sun and R. J. Bartlett, J. Chem. Phys. **104**, 8553 (1996).
- ⁵²W. Förner, R. Knab, J. Cizek, and J. Ladik, J. Chem. Phys. **106**, 10248 (1997).
- ⁵³M. Rohlfing and S. G. Louie, Phys. Rev. Lett. **82**, 1959 (1999).
- ⁵⁴P. Y. Ayala, K. N. Kudin, and G. E. Scuseria, J. Chem. Phys. **115**, 9698 (2001).
- ⁵⁵V. Bezugly and U. Birkenheuer, Chem. Phys. Lett. **399**, 57 (2004).
- ⁵⁶C. R. Fincher Jr., M. Ozaki, M. Tanaka, D. Peebles, L. Lauchlan, A. J. Heeger, and A. G. MacDiarmid, Phys. Rev. B **20**, 1589 (1979).
- ⁵⁷G. Leising, Phys. Rev. B **38**, 10313 (1988).
- ⁵⁸R. T. Sharp and G. K. Horton, Phys. Rev. **90**, 317 (1953).
- ⁵⁹J. B. Krieger, Y. Li, and G. J. Iafrate, Phys. Lett. A **146**, 256 (1990).
- ⁶⁰E. Engel and S. H. Vosko, Phys. Rev. A **47**, 2800 (1993).
- ⁶¹A. Görling and M. Levy, Phys. Rev. A **50**, 196 (1994).
- ⁶²A. Görling and M. Levy, Int. J. Quantum Chem. **29**, 93 (1995).
- ⁶³H. J. Monkhorst and J. D. Pack, Phys. Rev. B **13**, 5188 (1976).
- ⁶⁴S. Froyen, Phys. Rev. B **39**, 3168 (1989).
- ⁶⁵D. M. Bylander and L. Kleinman, Phys. Rev. Lett. **74**, 3660 (1995); Phys. Rev. B **52**, 14566 (1995); Phys. Rev. B **54**, 7891 (1996); **55**, 9432 (1997).
- ⁶⁶M. Moukara, M. Städele, J. A. Majewski, P. Vogl, and A. Görling, J. Phys.: Condens. Matter **12**, 6783 (2000).
- ⁶⁷D. R. Hamann, M. Schlüter, and C. Chiang, Phys. Rev. Lett. **43**, 1494 (1979); G. B. Bachelet, D. R. Hamann, and M. Schlüter, Phys. Rev. B **26**, 4199 (1982).
- ⁶⁸D. R. Hamann, Phys. Rev. B **40**, 2980 (1989).
- ⁶⁹N. Troullier and J. L. Martins, Phys. Rev. B **43**, 1993 (1991).
- ⁷⁰E. Engel, A. Höck, R. N. Schmid, R. M. Dreizler, and N. Chetty, Phys. Rev. B **64**, 125111 (2001).
- ⁷¹C. S. Yannoni and T. C. Clarke, Phys. Rev. Lett. **51**, 1191 (1983).